NEUVIEME COLLOQUE SUR LE TRAITEMENT DU
SIGNAL ET SES APPLICATIONS

NICE du 16 au 20 MAI 1983

THE METHOD OF PROJECTIONS ONTO CONVEX SETS (POCS) FOR RESTORING IMAGES FROM INCOMPLETE INFORMATION

H. Stark, I.M. Sezan, and A. Levi

ECSE DEPART. RENSSELAER POLYTECHNIC INST., TROY, N.Y. 12181, USA

RESUME

Dans cet article on utilise la méthode de projection sur les ensembles convexes (appellé POCS) pour rétablir les images à partir de l'information incomplète. La methode POCS est equivalent à trouver un point de l'intersection de m ensembles convexes, où m est le nombre de propriétes de l'image connues à priori. On démontre comment la methode POCS est utilisée pour retablir les images a partir de 1. l'information incomplète dans l'espace de Fourier et 2. l'information dans l'espace de phase suelement.

SUMMARY

In this paper, we apply the method of projections onto convex sets (POCS) for restoring images from incomplete information. The method of POCS is equivalent to finding a point that lies at the intersection of m convex sets where m is the number of a priori-known properties of the image. We shall show how POCS is used in restoring images from 1. incomplete Fourier-space information and 2. phase information only.

THE METHOD OF PROJECTIONS ONTO CONVEX SETS (POCS) FOR RESTORING IMAGES FROM INCOMPLETE INFORMATION

H. Stark, I.M. Sezan, and A. Levi

INTRODUCTION

In several important practical situations it is required to restore a signal or image from incomplete information. The problem of reconstructing a tomographic image from partial view data is one of them. Besides the well-known medical applications in computerized tomography (CT) there is also a wide range of nonmedical applications in meteorology, electron microscopy, geophysics, astronomy, and oceanography which require construction of an image from partial information. For this reason Gerchberg-Papoulis (GP) algorithms [2], [3], [6], and their offsprings [4], [5] have generated considerable interest.

The method of projections onto convex sets (POCS) [1] has a significant advantage over the GP and related algorithms in that it enables a large number of a priori known constraints to be incorporated in the algorithm provided that they are formulated as constraints that restrict the image function to lie in a closed convex set. Not every constraint can be viewed as a restriction in terms of convex sets. For example the operation of digitizing a signal is not equivalent to projection onto a convex set. However numerous other constraints can be treated as convex set restrictions and we shall illustrate this with examples. Eleven signal and image constraints and their associated projection operators are furnished in [7] and many of those are of physical significance.

METHOD OF PROJECTIONS ONTO CONVEX SETS (POCS)

The basic idea in POCS is the following: Every a priori known property of an unknown image function $f \epsilon \mathcal{H}$ ($\mathcal{H}$ a Hilbert space) is viewed as a constraint that restricts the signal to lie in a well known closed convex set C_i. Thus for m properties, there are m sets C_i i=1, 2, ..., m and the function f must lie in the intersection $C_0 = \bigcap_{i=1}^{m} C_i$. The problem is then to find a point of C_0 given the sets C_i and the operators P_i, i=1, 2, ..., m that project onto the $\{C_i\}$. Given an arbitrary $f \epsilon \mathcal{H}$, its projection onto C_i is that element h that satisfies.

$$\min_{y \epsilon C_i} ||f-y|| = ||f-h||. \tag{1}$$

The restoration algorithm that "finds" a point of C_o has the form

$$f_{k+1} = P_m P_{m-1} \cdots P_1 f_k \quad k=0, 1, 2, \ldots \tag{2}$$

with f_o arbitrary. More generally, we can write

$$f_{k+1} = T_m T_{m-1} \cdots T_1 f_k \quad k=0, 1, 2, \ldots \tag{3}$$

where $T_i \overset{\Delta}{=} 1+\lambda_i(P_i-1)$ and $0<\lambda_i<2$. The relaxation parameter λ_i can be used to accelerate the rate of convergence both initially and in the vicinity of solution. The theoretical basis of the algorithm is given in [7], [10]. In general convergence to an $f \epsilon C_0$ is weak.

Because we shall deal with space-limited objects, defined by their reflectance, transmittance, or absorbtance over a region Ω, the functions of interest in this study will be assumed to be members of $L_{2x2}(\Omega)$, the space of all functions f(x,y) square-integrable over Ω. The associated Hilbert space $\mathcal{H}$ is $L_{2x2}(\Omega)$ with inner product and norm defined by, respectively,

$$(g,h) \overset{\Delta}{=} \iint_{\Omega} g(x,y)h^*(x,y)\, dxdy \tag{4}$$

$$||g|| \overset{\Delta}{=} [(g,g)]^{1/2} \tag{5}$$

In this paper we briefly demonstrate the application of the method of POCS to 1) reconstruction in CT from partial view data (Limited angular view problem) and 2) reconstruction of the magnitude of the Fourier transform from phase.

APPLICATION OF POCS IN CT

In CT by Direct Fourier reconstruction method (DFM), each view gives the projection data from which a single central slice of the discrete Fourier transform (DFT) is obtained. When all the views are obtained, the Fourier transform plane is packed with the Fourier data on a polar raster. After interpolation to a cartesian format as described in [8], an inverse 2-D DFT is computed which yields the desired image. But in the case of incomplete view data the known Fourier data will be in a data cone with subtended angle of <180°. The following sets and associated projection operators express some a priori known properties of the image function. These are significant in CT.

1. C_1: The set of all functions that vanish a•e outside a prescribed region $\mathcal{S} \subset \Omega$. Given an arbitrary $f \epsilon \mathcal{H}$ its projection onto C_1 is realized by

$$P_1 f = \begin{cases} f, & (x,y) \epsilon \mathcal{S} \\ 0, & (x,y) \notin \mathcal{S} \end{cases} \tag{6}$$

2. C_2: The set of all functions in $\mathcal{H}$ whose Fourier transforms assume a prescribed value G over a closed region L in the u-v Fourier plane. The projection of an arbitrary $f \epsilon \mathcal{H}$ onto C_2 is realized by

$$P_2 f \leftrightarrow \begin{cases} G(u,v) & (u,v) \epsilon L \\ F(u,v) & (u,v) \notin L \end{cases}, \tag{7}$$

where $F(u,v)=\mathcal{F}[f(x,y)]$ etc. for G(u,v) and $\mathcal{F}$ is the Fourier transform operator. In particular G(u,v) is the known portion of the spectrum of f over the data cone.

3. C_3: The set of all nonnegative real functions in $\mathcal{H}$ that satisfy the energy constraint

$$\iint_{\Omega} |f(x,y)|^2\, dxdy \le E \overset{\Delta}{=} \rho^2 \tag{8}$$

The projection of an arbitrary $f \epsilon \mathcal{H}$ onto C_3 is realized by

$$P_3 f = \begin{cases} 0 & f_1 < 0 \\ f_1^+ & E_1^+ \le E \\ \sqrt{\dfrac{E}{E_1^+}} \bullet f_1^+, & E_1^+ > E \end{cases} \tag{9}$$

where f_1 is the real part of f, f_1^+ is the rectified portion of f_1, and E_1^+ is the energy in f_1^+; i.e.,

$$E_1^+ \overset{\Delta}{=} \iint_{\Omega} (f_1^+)^2\, dxdy. \tag{10}$$

4. C_4: The subset of all functions in $\mathcal{H}$ that are nonnegative. The projection of an arbitrary $f \epsilon \mathcal{H}$ onto C_4 is realized by

$$P_4 f = \begin{cases} f_1 & f_1 \geq 0 \quad (f=f_1+jf_2) \\ 0, & \text{otherwise.} \end{cases} \tag{11}$$

5. C_5: The set of all real functions in H whose amplitudes must lie in a prescribed closed interval [a, b] $a \geq 0$, $b>0$, $a<b$. The projection onto C_5 is realized by the following rule:

$$P_5 f = \begin{cases} a & f_1(x,y) < a \\ f_1(x,y) & a \leq f_1(x,y) \leq b \\ b & f_1(x,y) > b. \end{cases} \tag{12}$$

In the above, $f \triangleq f_1+jf_2$.

Simulation of Limited Angular View Problem

The simulated image consists of three nested rectangles the longest being 24x32 pixels, centered on a 64x64 pixel field; it is shown in Fig. 1. The object is represented by a sequence, $f(m,n)$, $m=1, 2, \ldots, N$, $n=1\ldots, N (N=64)$ which represents the gray levels of the mn th pixel. The gray levels are confined to $0 \leq f(m,n) \leq 1$ and are 0.4, 0.8, and 1.0 in going from the largest to the smallest rectangle, respectively. The background level is zero.

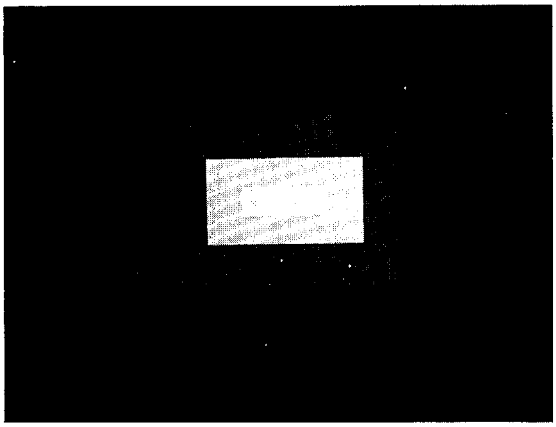

Fig. 1. The image: it consists of three nested rectangles of gray levels 1.0 (center), 0.8 and 0.4.

In our simulation a 90 degree data cone is used in all the experiments. We now summarize some a priori known facts and assumptions about the image.

A Priori Constraints	Actual
1) Image support confined to rectangular region $\Delta x=55$ pixels, $\Delta y=57$ pixels.	1) Image support in rectangular region $\Delta x=32$ pixels, $\Delta y=24$ pixels.
2) Gray levels f satisfy $0 \leq f \leq 1$.	2) Gray levels f satisfy $0 \leq f \leq 1$.
3) Energy over 64x64 pixel^2 field cannot exceed $\rho^2=268.5$.	3) Energy in object is 267.0 over the 32x24 pixel^2 object field. No energy outside.
4) Initially known spectrum $G(u,v)=F(u,v)\chi_c(\theta)$4) ($\chi_c(\theta)$ is 90° cone).	4) Spectrum of the image is $F(u,v)$.

The formula used for computing energy is

$$E \triangleq \sum_{m=1}^{64} \sum_{n=1}^{64} f^2(m,n)=267.$$

Algorithms

The following algorithms are implemented by a flexible program called PROCON whose description is given in [9].

1) Gerchberg-Papoulis (GP): The familiar G-P algorithm can be written in compact form, for our problem, as

$$f_{k+1}=P_2P_1f_k. \tag{13}$$

2) UNIRELAX 1: $f_{k+1}=P_2P_3P_1f_k$ (14)

3) RELAX 1: $f_{k+1}=T_2T_3T_1f_k$ with (15)

$\lambda_2=1.75$, $\lambda_3=\lambda_1=1.9995$.

Results

Figure 2 shows the reconstruction error as a function of iteration number k for GP, UNIRELAX 1 and RELAX 1. As can be seen both UNIRELAX 1 and RELAX 1, using the method of POCS significantly outperform the GP algorithm.

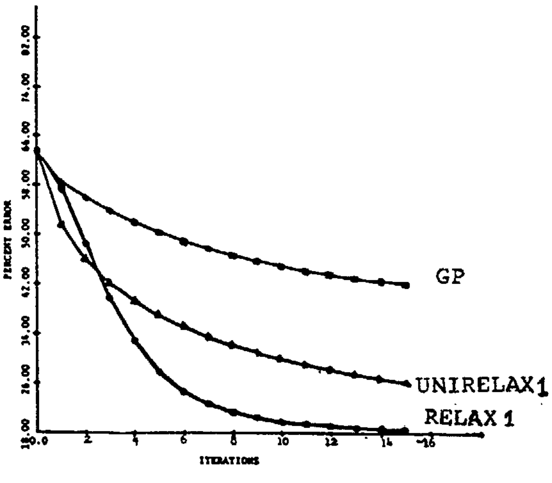

Fig. 2. Error versus iteration number k for GP, UNIRELAX 1, and RELAX 1.

In Fig. 3 are shown the actual restorations from the 90 degree data cone after 30 iterations.

Figure 3 furnishes impressive evidence that methods based on projections onto convex sets furnish markedly superior restorations to the Gerchberg-Papoulis method.

We note that projections onto C_4 and C_5 do not appear in Eqs. (14) or (15). First of all since C_5 C_4 it follows that P_5 (or T_5) would be more likely to restrict the solution set than P_4 (or T_4). However when P_5 (T_5) was actually used its affect was negligible so that we ignored it in the results presented here.

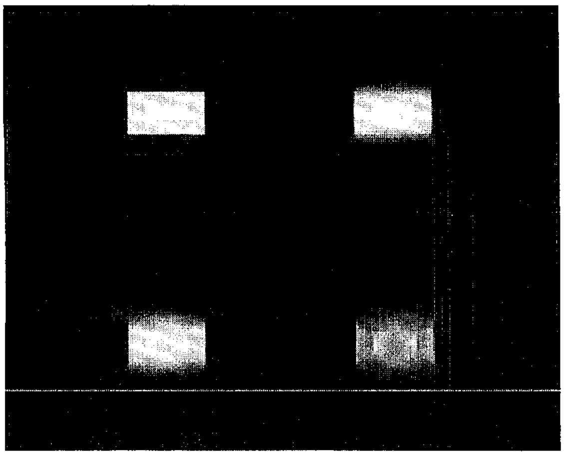

Fig. 3. Restoration of the image. Counterclockwise from upper left: original object, UNIRELAX 1, GP, RELAX 1.

RESTORATION FROM PHASE (RFP) BY POCS

The two sets of principal interest in the restoration-from-phase (RFP) problem are

$$C_1 = \{f(x) : f(x)=0, \ |x| > a\} \tag{16}$$

and

$$C_2 = \{f(x) : \arg[F(\omega)] = \phi(\omega)\}. \tag{17}$$

In words: C_1 is the set of space-truncated functions and C_2 is the set of all f's ϵH with prescribed phase. Both C_1 and C_2 are closed convex sets. With P_i denoting the projection operator onto C_i, it is not difficult to show that P_1 and P_2 are realized by

$$P_1 f = \begin{cases} f(x) & , |x| \le a \\ 0 & , |x| > a \end{cases} \tag{18}$$

and

$$P_2 f = \begin{cases} |F(\omega)|\cos[\phi(\omega)-\psi(\omega)]e^{j\phi(\omega)} & , \omega\epsilon\Omega \\ 0 & , \omega\epsilon\Omega^c \end{cases} \tag{19}$$

where $\phi(\omega)$ is the prescribed phase, $f(x)$ is an arbitrary element of H and $|F(\omega)|e^{j\psi(\omega)}$ is the Fourier transform of $f(x)$. Ω is the set given by

$$\Omega = \{\omega: \cos[\phi(\omega)-\psi(\omega)] \ge 0\} \tag{20}$$

and Ω^c by

$$\Omega^c = \{\omega: \cos[\phi(\omega)-\psi(\omega)] < 0\} \tag{21}$$

i.e., the complement of Ω. As defined, P_2 is a non-linear operator while P_1 is linear. From now on we shall use the following notation
$f(x) \leftrightarrow F(\omega)=|F(\omega)|e^{j\phi(\omega)}$ is a Fourier transform (FT) pair representing a point in $C_0 = C_1 \cap C_2$.
$f(x) \leftrightarrow |F_n(\omega)|e^{j\psi_n(\omega)}$ is a FT pair representing the estimate of $f(x)$ at the n'th iteration.

Optimization of the Two-Step POCS

Let f be a point in C_0. We define the error after the n'th iteration by

$$e_n \triangleq f_n - f. \tag{22}$$

We consider the per-cycle optimization of the λ's. By per-cycle optimization we mean the following: For a given f_n find λ_{1m} and λ_{2m} such that $||e_{n+1}||$ is minimum. This method is described in detail in [11]. In the general case when P_2 is a non-linear operator λ_{1m} can be approximated by 1) minimizing an approximate expression for the error $||e_{n+1}||^2$, or 2) minimizing the expression

$$I \triangleq -\lambda_1(2-\lambda_1)||P_1 f_n - f_n||^2 - ||P_2 T_1 f_n - T_1 f_n||^2 \tag{23}$$

which is equivalent to minimizing some upper bound of $||e_{n+1}||^2$. This minimization can be done by a straightforward scan through the range of λ_1. Then, having obtained an approximate λ_{1m}, we compute λ_{2m} from

$$\lambda_{2m} = \frac{\mathrm{Re}[(f-T_1 f_n, \ P_2 T_1 f_n - T_1 f_n)]}{||P_2 T_1 f_n - T_1 f_n||^2}, \tag{24}$$

where (x,y) for any $x,y\epsilon H$ means the inner product in the Hilbert space H. Since f is unknown we use f_n to calculate the unknown part of f. A similar technique is used when λ_{1m} is determined by 1). In the case where P_2 is a linear operator we can show that $\lambda_{2m}=1$ and we can obtain a closed form solution for λ_{1m}. We consider two possible commutations for the RFP problem:

(a) $f_{n+1}=T_2T_1f_n$

As already stated, since P_2 is non-linear we can find λ_{1m} by either 1) minimizing some approximate expression for the error $||e_{n+1}||^2$ (not given here because of space limitations), or 2) minimizing I in Eq. (23) using a scan through some range of λ_1. λ_{2m} can be found from Eq. (24) after calculating λ_{1m}. When Eq. (24) is written in the transform domain we can approximate the unknown amplitude $|F(\omega)|$ by the best estimate of it that we have namely $|F_n(\omega)|$.

(b): $f_{n+1} = T_1T_2f_n$

In this case the last operator in the cycle is linear and it can be shown [11] that

$$\lambda_{1m}=1 \tag{25}$$

and

$$\lambda_{2m}=1+\frac{||P_2f_n-P_1P_2f_n||^2}{||P_1P_2f_n-f_n||^2}+\frac{\mathrm{Re}[(f-P_2f_n, \ P_2f_n-f_n)]}{||P_1P_2f_n-f_n||^2} \tag{26}$$

the last term on the right in Eq. (26) is always positive and can be either 1) approximated by using its Fourier transform domain equivalent form and replacing $|F(\omega)|$ by $|F_n(\omega)|$, or 2) neglected. When the last term on the right of Eq. (26) is neglected the resulting λ_{2m} is actually a lower bound. Results using this lower bound (subject to it not exceeding the value of 2) is given in the example.

EXAMPLE

The example given in this paper shows the dependence of the restoration on the initialization, the number of iterations and on the optimization of the λ's. The original signal to be restored from phase-only is given in Fig. 4 and the results for the different cases are summarized in tables 1 and 2. The error given in the tables is a per-cent error defined by

$$e_n = 100 \cdot \frac{||f_n - f||}{||f||} \qquad (27)$$

The signal to be restored is a truncated 128 point cosine on a pedestal given by

$$f(x) = \begin{cases} 0.5+0.5\cos(\pi x/30), & x=1, \ldots, 50 \\ 0, & x=51, \ldots, 128 \end{cases} \qquad (28)$$

In tables 1 and 2 F_o denotes the initial arbitrary value of the Fourier transform magnitude (this is an input to the program furnished by the user). Table 1 gives the results for F_o=10, and table 2 for $F_o=10\exp(-\omega^2/100)$, where ω=0, 1, 2, ... (i.e., is discrete). The main conclusions drawn from these tables are:

- The method of POCS effectively restores the signal even with no optimization of the λ's.
- The results depend strongly on the initialization F_o.
- Per-cycle optimization of the λ's significantly improves restoration over pure projections ($\lambda_1=\lambda_2=1$). For the same final error and with no optimization we need at least twice the number of iterations that we need with optimization.
- The order in which the operators are applied does affect the rapidity of convergence. A "best" ordering procedure is not, at present, known.
- Because of the importances of good initialization, one should attempt to obtain or use a priori information that will get F_o as close to $F(\omega)$ as possible.

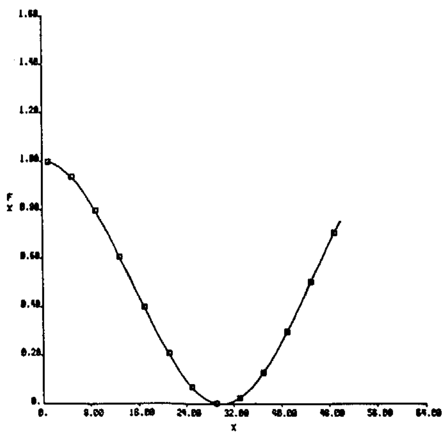

Fig. 4. Original signal to be restored from phase-only.

Table 1
F_o=10

Iteration Number	$\lambda_1=\lambda_2$=1.0	Optimization for $f_{n+1}=T_2T_1f_n$	Optimization for $f_{n+1}=T_1T_2f_n$
0	79.9	79.9	79.9
1	68.1	39.2	61.3
2	60.3	26.3	49.1
3	54.1	21.9	41.9
5	45.2	16.2	33.6
10	34.2	10.7	23.2
15	28.3	7.4	17.1
20	24.0	5.3	12.9
25	20.6	3.9	9.8
30	17.8	2.9	7.6
35	15.4	2.2	5.9
39	13.8	1.8	4.8
99	3.0		

Table 2
$F_o=10\exp[-\omega^2/100]$

Iteration	$\lambda_1=\lambda_2$=1.0	Optimization for $f_{n+1}=T_2T_1f_n$	Optimization for $f_{n+1}=T_1T_2f_n$
0	26.1	26.1	26.1
1	18.3	17.4	15.1
2	15.4	14.1	13.2
3	14.1	12.7	11.9
5	12.5	10.4	9.7
10	9.7	6.9	6.5
15	7.8	4.9	4.7
20	6.5	3.7	3.5
25	5.4	2.9	2.7
30	4.7	2.2	2.1
35	4.0	1.7	1.6
39	3.6	1.4	1.3

CONCLUSIONS

In this paper we discussed the applications of the method of POCS to 1) CT image restoration and 2) the restoration-from-phase problem. In general the method allows for any number of a priori known image constraints to be incorporated in the algorithm provided that these can be associated with convex sets. We discussed methods of approximately optimizing the relaxation parameters and showed thereby that a significant improvement in performance can be obtained. This algorithm has the property of guaranteed convergence (strong convergence in the finite-dimensional case) with and without the use of relaxation parameters.

ACKNOWLEDGEMENTS

This work was supported in part by National Science Foundation Grant ECS 8111265 and by RADC (Rome, New York) contract F3060282K0151.

REFERENCES

[1] M.I. Sezan and H. Stark, "Image Restoration by the Method of Convex Projections: Part 2 - Applications and Numerical Results", IEEE Trans on Medical Imaging Vol. MI-1, No. 2, October 1982.

[2] R.W. Gerchberg, "Super-resolution through error reduction," Opt. Acta, vol. 21, pp. 709-720, 1974.

[3] A. Papoulis, "A new algorithm in spectral analysis and band-limited extrapolation," IEEE Trans. Circuits Syst., vol. CAS-22, pp. 735-742, 1975.

[4] H. Stark, D. Cahana, and H. Webb, "Restoration of arbitrary finite-energy optical objects from limited spatial and spectral information," J. Opt. Soc. Amer., vol. 71, no. 6, pp. 635-642, 1981.

[5] J.A. Cadzow, "An extrapolation procedure for band-limited signal extrapolation: The extrapolation: The extrapolation matrix," IEEE Trans. Circuists Syst., vol. CAS-25, pp. 74-78, 1978.

[6] D.C. Youla, "Generalized image restoration by the method of alternating projections," IEEE Trans. Circuits Syst., vol. CAS-25, pp. 694-702, 1978.

[7] D.C. Youla and H. Webb, "Image restoration by the method of convex projections: Part 1 - Theory," IEEE Trans on Medical Imaging Vol. MI-1, No. 2, October 1982.

[8] H. Stark, J.W. Woods, I. Paul, and R. Hingorani, "Direct Fourier reconstruction in computer tomography," IEEE Trans. Acoust., Speech, Signal Processing, vol. ASSP-29, pp. 237-245, 1981.

[9] M.I. Sezan and H. Stark, "An investigation of image restoration by projections onto convex sets," Image Processing Lab., Rensselaer Polytechnic Institute, Rep. IPL-TR-031.

[10] L.G. Gubin, B.T. Polyak, and E.V. Raik, "The method of projections for finding the common point of convex sets," U.S.S.R. Comput. Math. and Math. Phys., vol. 7, no. 6, pp. 1-24, 1967.

[11] A. Levi and H. Stark, "Signal Restoration from phase by Projections onto Convex Sets", to be published in the J. Opt. Soc. Am., May 1983.